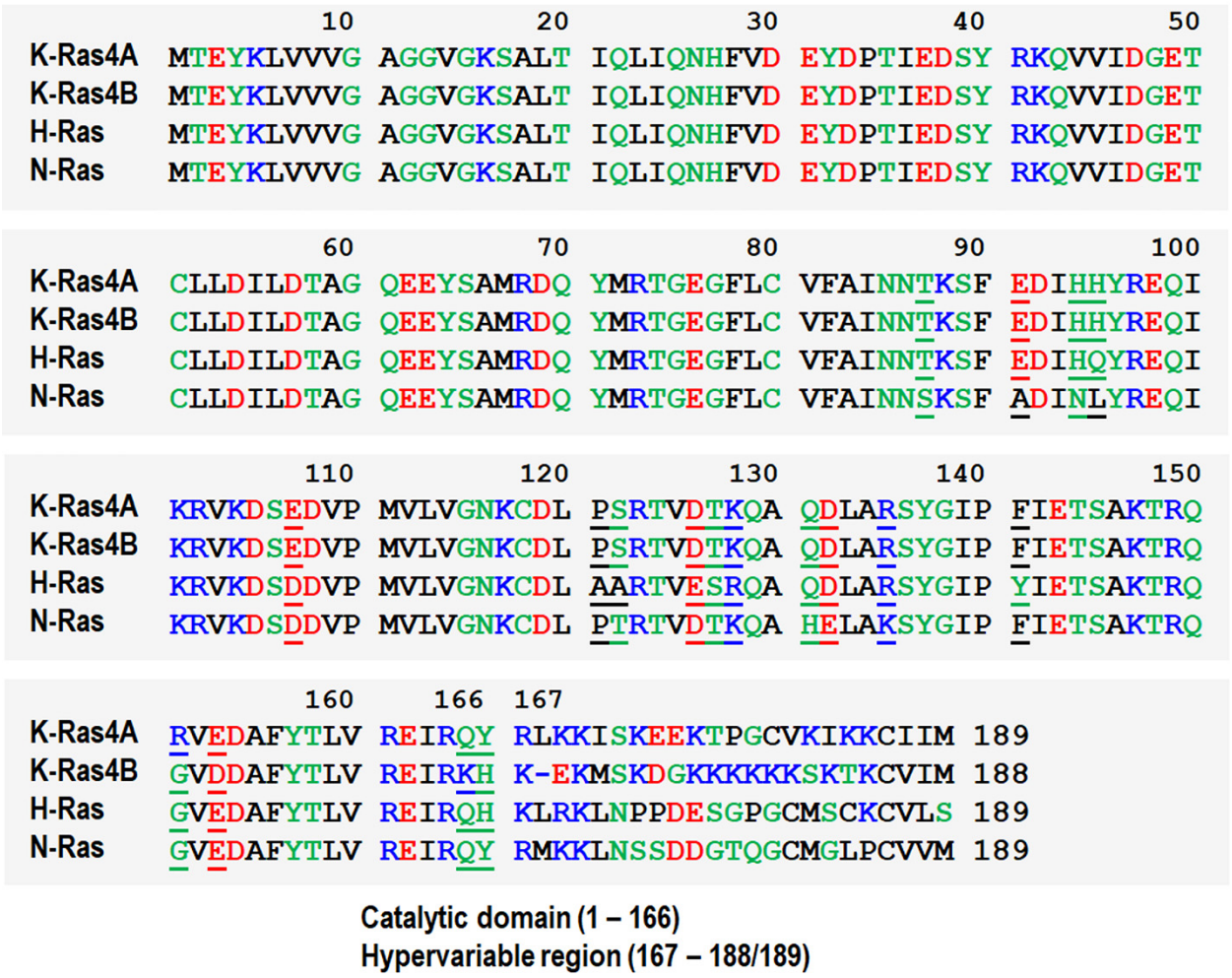

Figure S1. Multiple Sequence Alignment of the Amino Acids in KRas4A, KRas4B, HRas, and NRas. Related to Figure 1 and STAR methods section "Generating Initial Configurations of KRas4B–CaM Complex for Explicit MD Simulations".

In the sequence, hydrophobic, polar/glycine, positively charged, and negatively charged residues are colored black, green, blue, and red, respectively. The nonidentity of residues in the alignment is indicated by underlined texts.

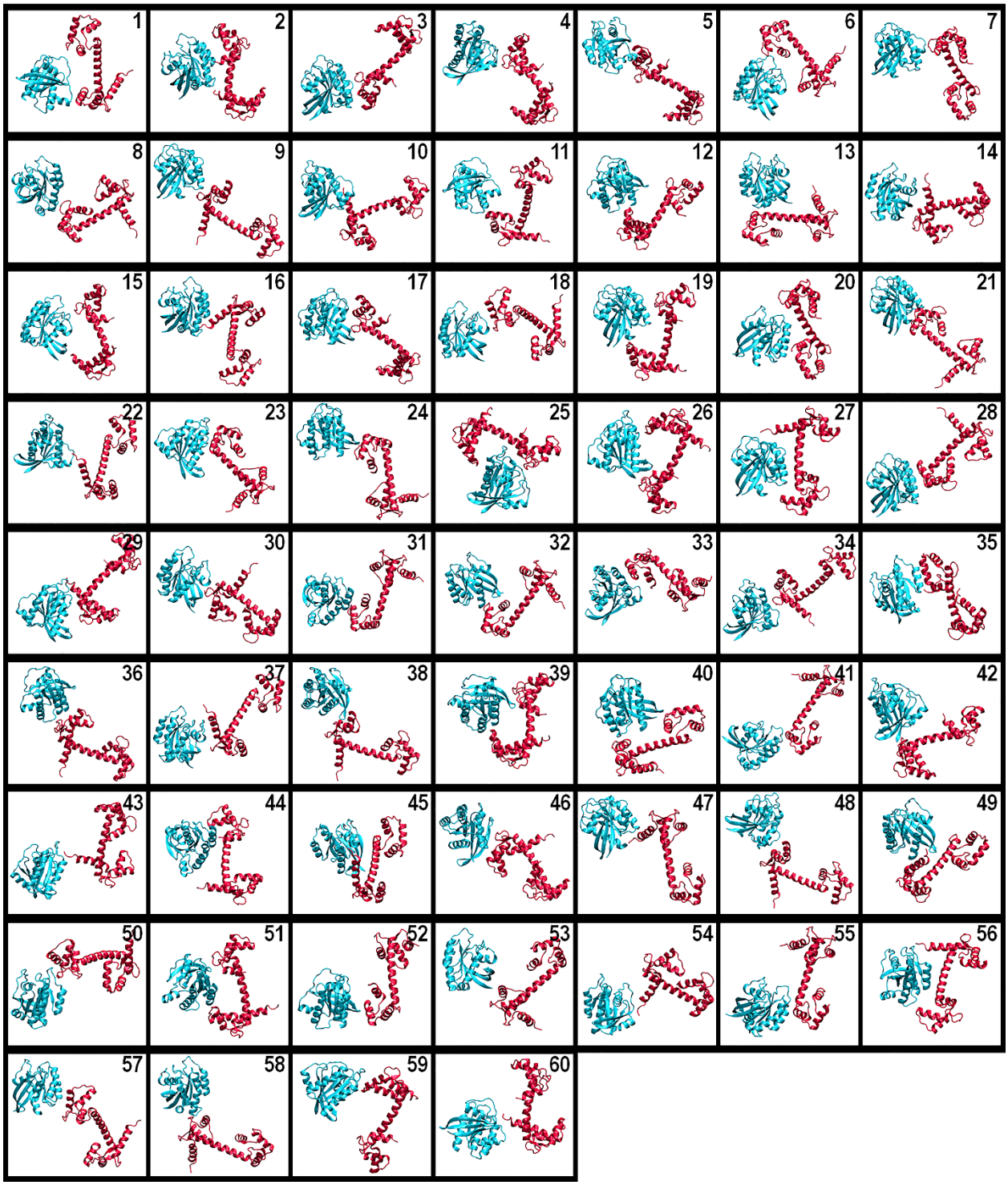

Figure S2. Predicted KRas4B$_{1\text{-}166}$–CaM Decoys with Extended CaM from the Rosetta Docking Program. Related to STAR methods section "Generating Initial Configurations of KRas4B–CaM Complex for Explicit MD Simulations".

The crystal structures of KRas4B$_{1\text{-}166}$ (PDB code: 3GFT) and CaM (PDB code: 1CLL) with a stretched linker were used for the docking.

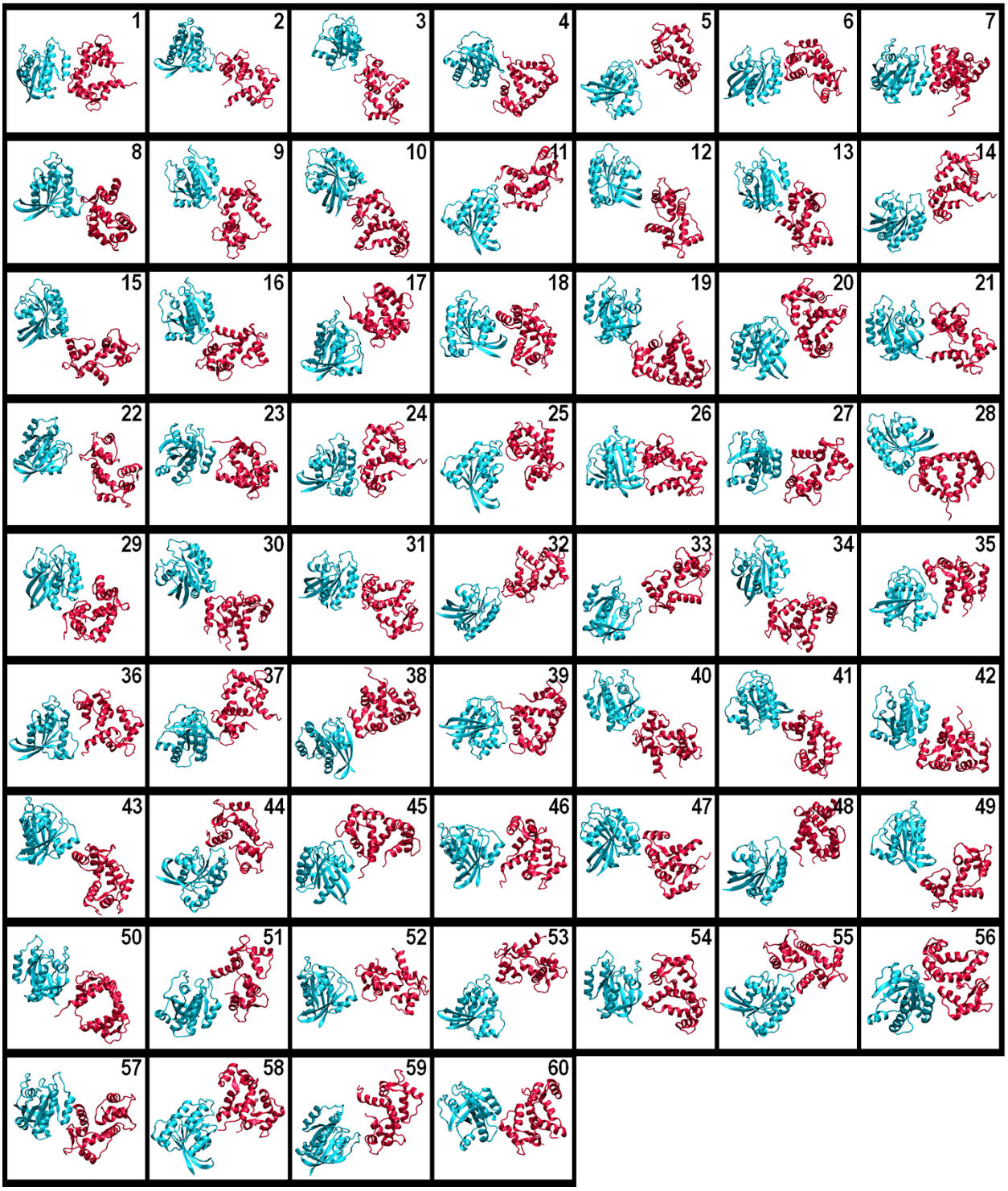

Figure S3. Predicted KRas4B$_{1\text{-}166}$–CaM Decoys with Collapsed CaM from the Rosetta Docking Program. Related to STAR methods section "Generating Initial Configurations of KRas4B–CaM Complex for Explicit MD Simulations".

The crystal structures of KRas4B$_{1\text{-}166}$ (PDB code: 3GFT) and CaM (PDB code: 1CDL) with a collapsed linker were used for the docking.

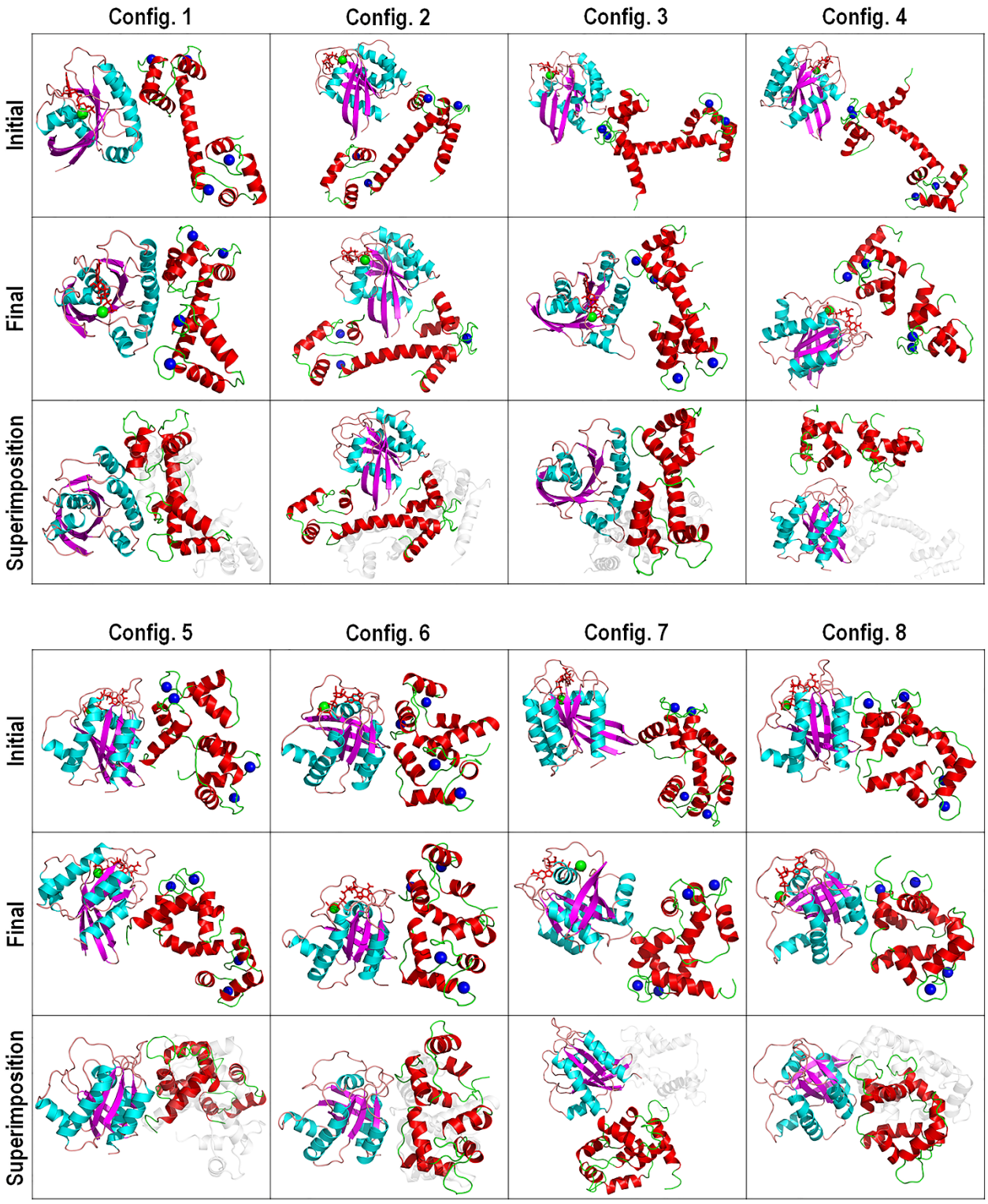

Figure S4. Simulated Configurations of KRas4B$_{1\text{-}166}$–CaM Complex. Related to Figure 2.
Snapshots representing the initial (upper panel of each configuration), final (middle panel of each configuration), and superimposition of the initial and final structures (lower panel of each configuration) for the truncated KRas4B$_{1\text{-}166}$–CaM complex. In the superimpositions, initial structures are shown as white transparent cartoons.

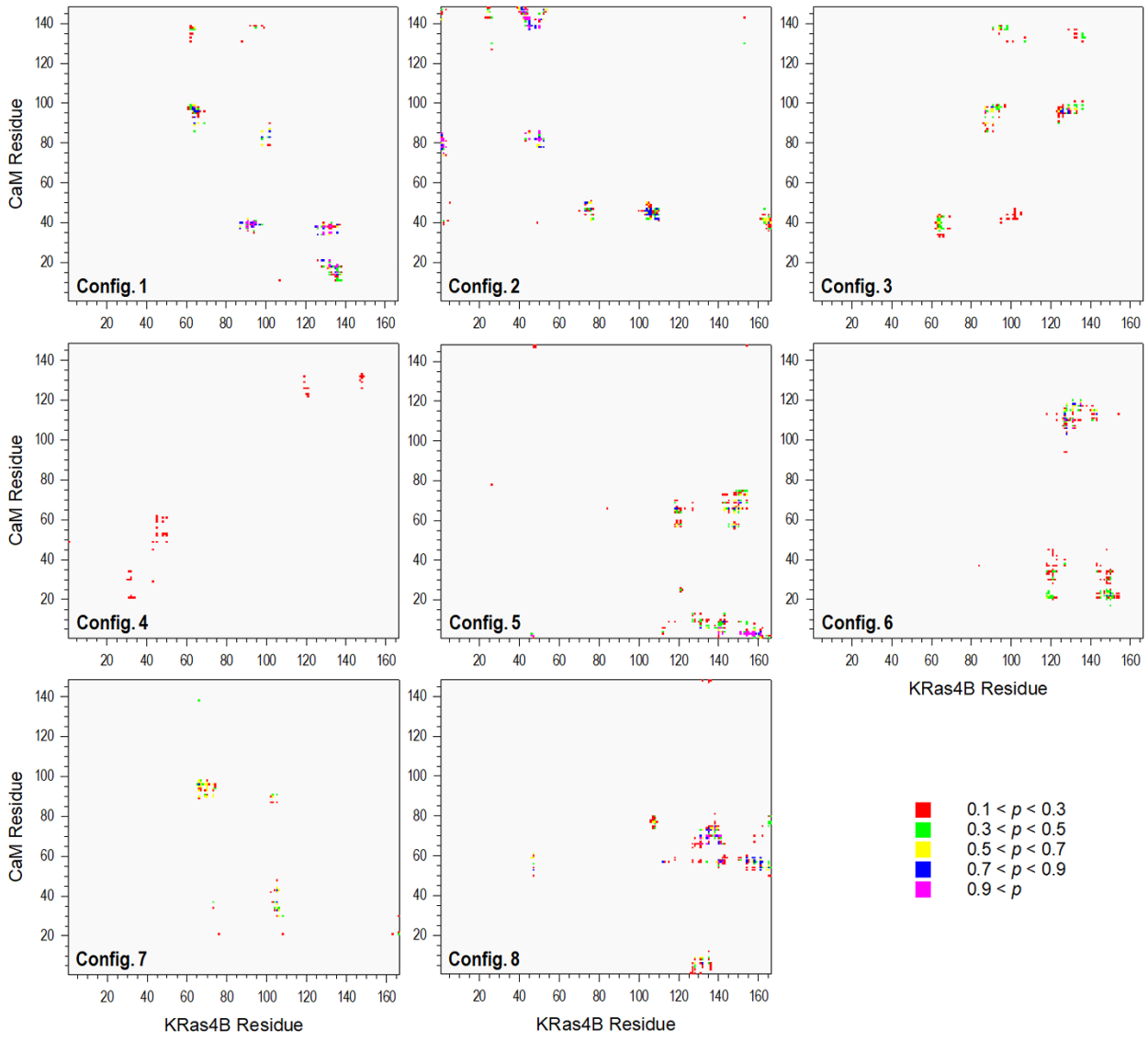

Figure S5. Intermolecular Residue-Residue Contacts Between Truncated KRas4B$_{1\text{-}166}$ and CaM. Related to Figure 2 and Figure 4.

For two intermolecular residues *i* and *j*, the probability of contact for the distance between the C_β^i–C_β^j atom (C_α is used for Gly residue) with cutoff 10 Å was calculated.

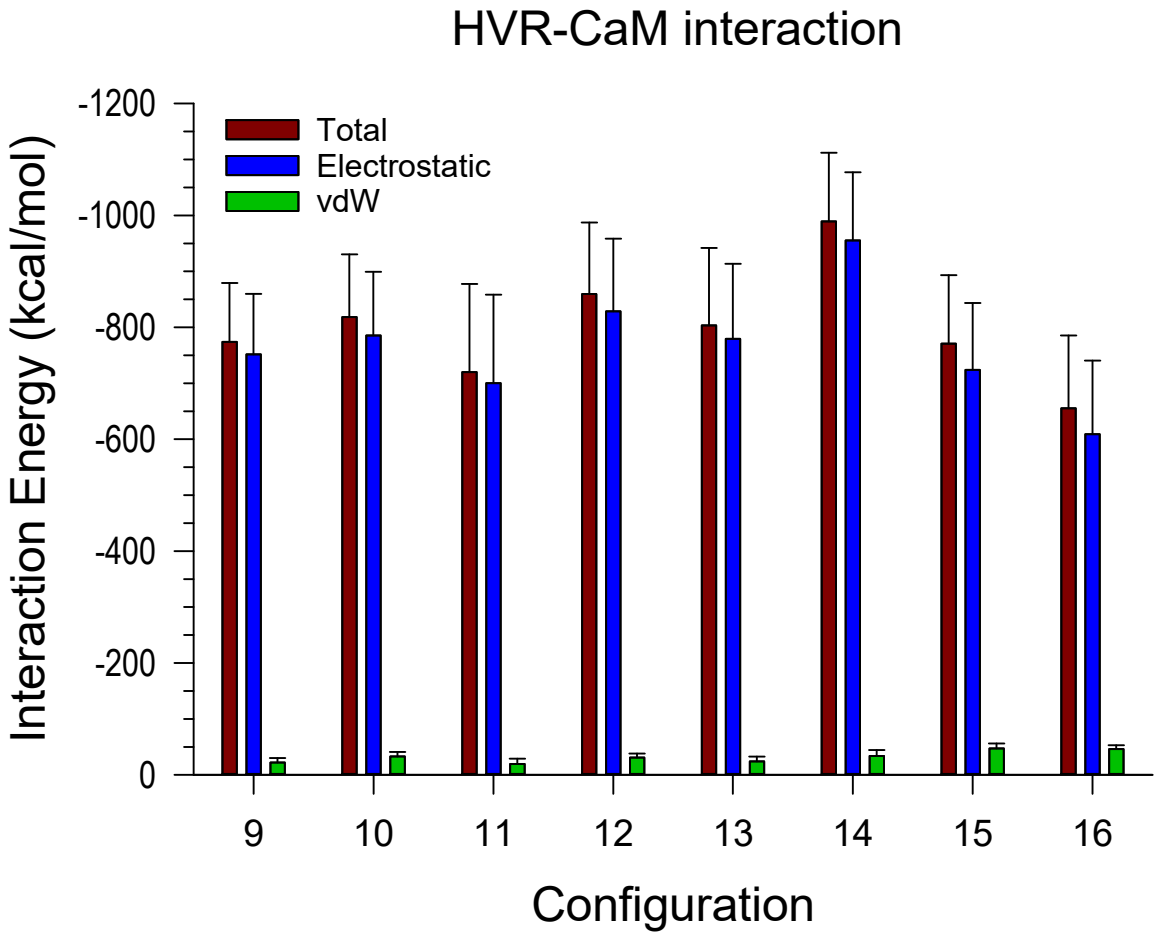

Figure S6. Averaged Interaction Energies of the HVR with CaM. Related to Figure 3 and Figure 5. The electrostatic and van der Waals (vdW) interactions contribute to the total interaction energy.

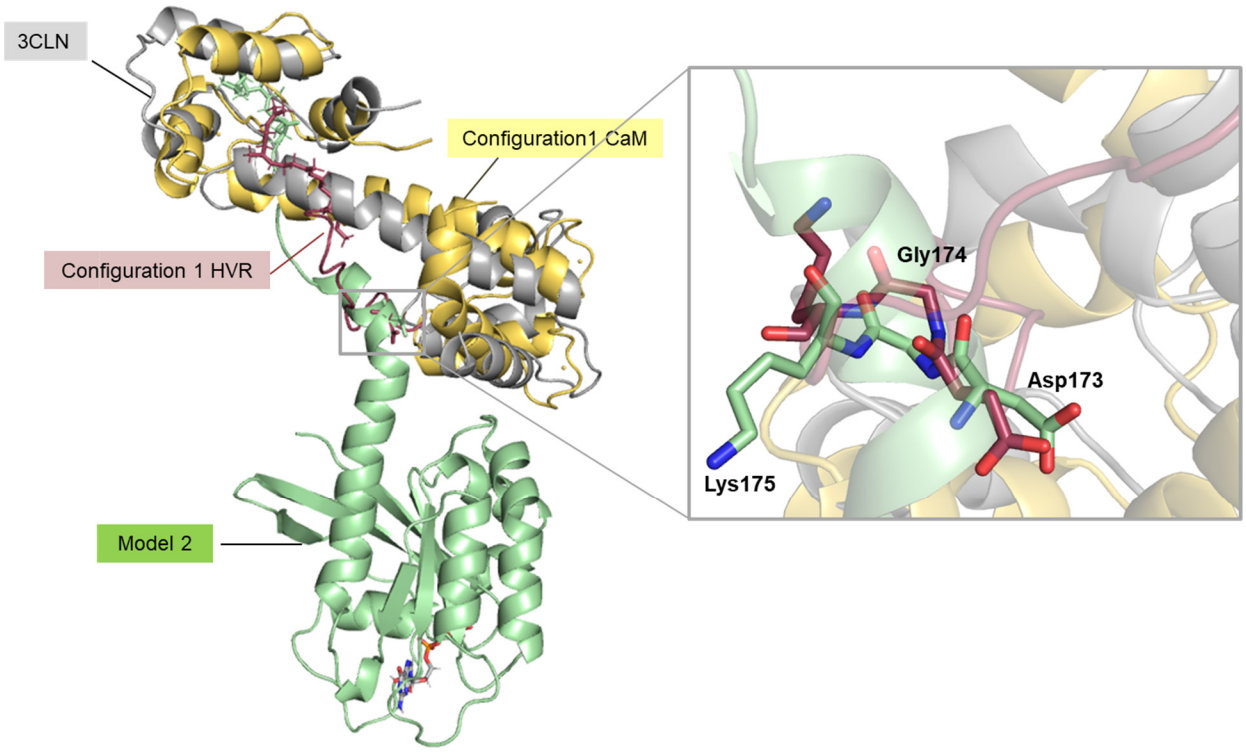

Figure S7. Generating SAXS Models. Related to Figure 6, Figure 7, and STAR methods section "Construction of SAXS Models for FME KRas4B–CaM Complex".
Alignment by CaM between the HVR structure (Config. 1 in ref. (Jang et al., 2017)) and Model 2 (SM-2). The CaM structure in SM-2 was aligned with that in Config. 1 of the HVR–CaM complex from previous studies (Jang et al., 2017) by doing a best fit superposition between the CaM molecules of each model. It was found that residues 173-175 from both models aligned in nearly identical locations. Thus, the portion of the HVR C-terminal of residue 173 was removed from SM-2 and replaced by the HVR and CaM models from Config.1 of the HVR–CaM complex to create SM-3.

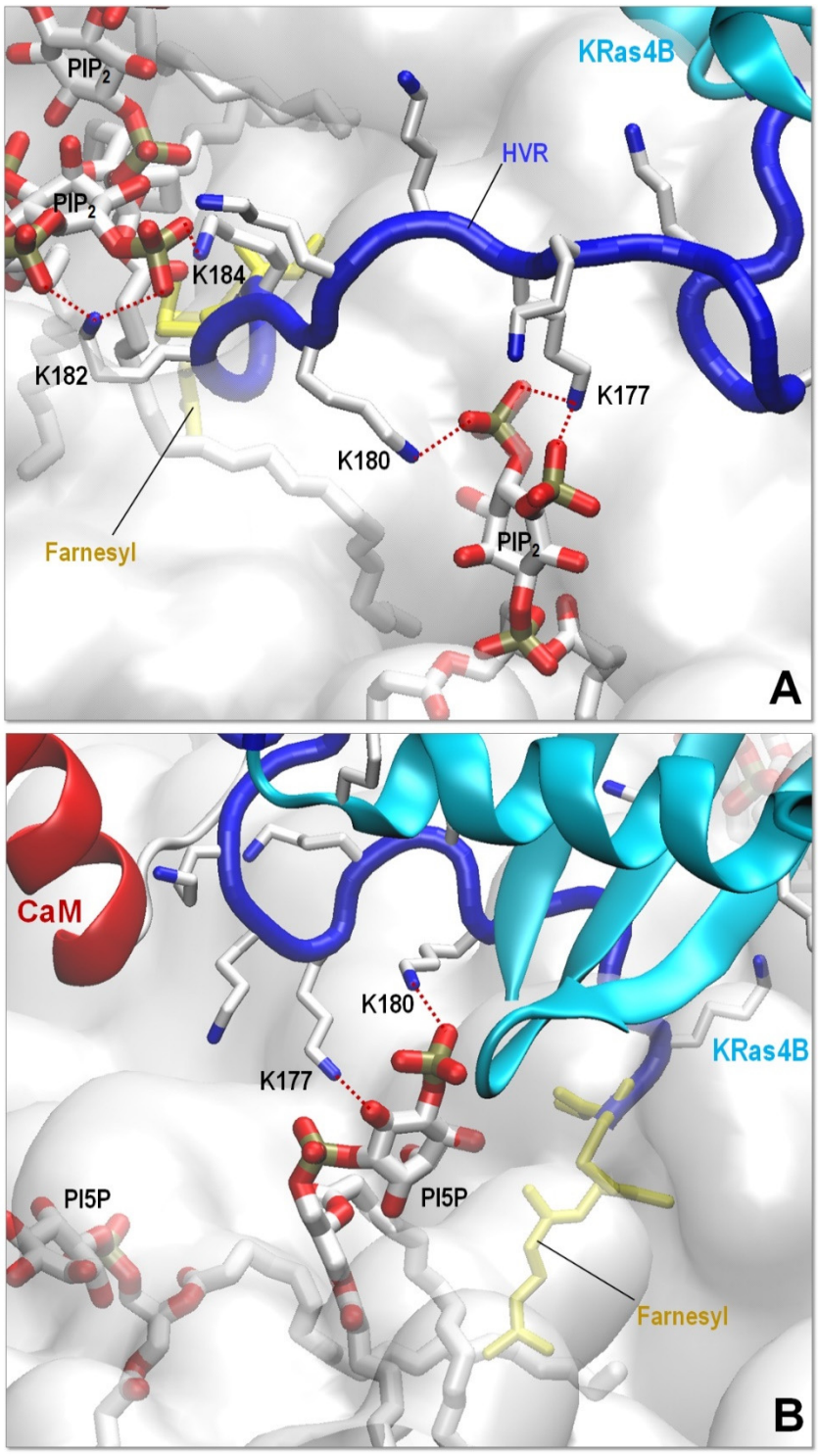

Figure S8. HVR Interaction with Signaling Lipids. Related to Figure 8 and Figure 9.
Snapshots depicting the interaction of the HVR lysine residues at the anchor region with signaling lipids at the (A) PIP_2 (DOPC:DOPS:PIP_2 with molar ratio 32:7:1) and (B) PI5P (DOPC:DOPS:PI5P with molar ratio 32:7:1) bilayers. Red dotted lines highlight the salt bridge interaction.